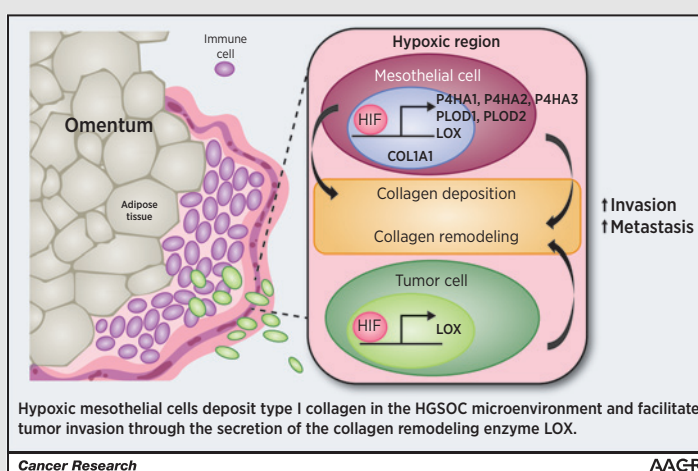**Tumor Biology and Immunology**

Cancer Research

Collagen Remodeling in the Hypoxic Tumor-Mesothelial Niche Promotes Ovarian Cancer Metastasis

Suchitra Natarajan[1], Kaitlyn M. Foreman[1], Michaela I. Soriano[1], Ninna S. Rossen[1,2], Hussein Shehade[1], Daniel R. Fregoso[1], Joshua T. Eggold[1], Venkatesh Krishnan[3], Oliver Dorigo[3], Adam J. Krieg[4], Sarah C. Heilshorn[2], Subarna Sinha[5], Katherine C. Fuh[6], and Erinn B. Rankin[1,3]

Abstract

Peritoneal metastases are the leading cause of morbidity and mortality in high-grade serous ovarian cancer (HGSOC). Accumulating evidence suggests that mesothelial cells are an important component of the metastatic microenvironment in HGSOC. However, the mechanisms by which mesothelial cells promote metastasis are unclear. Here, we report that the HGSOC tumor-mesothelial niche was hypoxic, and hypoxic signaling enhanced collagen I deposition by mesothelial cells. Specifically, hypoxic signaling increased expression of lysyl oxidase (LOX) in mesothelial and ovarian cancer cells to promote collagen cross-linking and tumor cell invasion. The mesothelial niche was enriched with fibrillar collagen in human and murine omental metastases. Pharmacologic inhibition of LOX reduced tumor burden and collagen remodeling in murine omental metastases. These findings highlight an important role for hypoxia and mesothelial cells in the modification of the extracellular matrix and tumor invasion in HGSOC.

Hypoxic mesothelial cells deposit type I collagen in the HGSOC microenvironment and facilitate tumor invasion through the secretion of the collagen remodeling enzyme LOX.

Significance: This study identifies HIF/LOX signaling as a potential therapeutic target to inhibit collagen remodeling and tumor progression in HGSOC.

Graphical Abstract: http://cancerres.aacrjournals.org/content/canres/79/9/2271/F1.large.jpg.

Introduction

Ovarian cancer is the fifth leading cause of cancer-related deaths among women in the United States. Despite advances in surgical and cytotoxic therapies, 80% of patients with advanced HGSOC develop recurrent, chemoresistant disease, resulting in a 5-year survival rate of 30% (1). The majority of women diagnosed with high-grade serous ovarian cancer (HGSOC) present with stage III or IV disease in which the tumor has disseminated beyond the ovaries and pelvic organs to the peritoneum and abdominal organs including the diaphragm, stomach, omentum, liver, and intestines. Peritoneal metastases significantly contribute to morbidity in patients with ovarian cancer as these tumors are numerous and often obstruct vital organs in the abdomen including the bowels (1). In addition, peritoneal metastases are associated with the formation of ascites that contribute to morbidity by increasing intra-abdominal pressure, leading to impaired circulation and respiratory distress (1). Therefore, understanding the fundamental mechanisms that drive ovarian peritoneal metastasis may lead to the development of effective therapies to reduce morbidity and mortality in patients with ovarian cancer.

[1]Department of Radiation Oncology, Stanford University, Palo Alto, California. [2]Department of Materials Science and Engineering, Stanford University, Palo Alto, California. [3]Department of Obstetrics and Gynecology, Stanford University, Palo Alto, California. [4]Oregon Health & Science University, Portland, Oregon. [5]SRI International, Menlo Park, California. [6]Division of Gynecologic Oncology, Washington University, St. Louis, Missouri.

Corresponding Author: Erinn B. Rankin, Stanford University, 269 Campus Drive, 1245 CCSR, Stanford, CA 94305. Phone: 650-497-8742; Fax: 650-723-1646; E-mail: erankin@stanford.edu

AACR 2271

The metastatic microenvironment in ovarian cancer is complex and dynamic with multiple cell types that support ovarian cancer metastasis. Among these cell types, mesothelial cells play an important role in the peritoneal metastatic niche. When establishing peritoneal implants, disseminated ovarian cancer cells migrate toward, attach, invade, and proliferate into the mesothelial cell layer covering the surface of organs in abdominal cavity including the omentum, a common site for ovarian cancer metastasis (2–4). Intraperitoneal injection of primary human peritoneal mesothelial cells with ovarian cancer cells increases peritoneal metastasis in immunodeficient mice compared with injection of tumor cells alone (5). Mesothelial cells promote HGSOC tumor cell adhesion, proliferation, and invasion, indicating that mesothelial cells play an active role in ovarian peritoneal metastasis (6, 7). However, little is known regarding the molecular mechanisms by which HGSOC tumor–mesothelial interactions promote metastasis.

Hypoxia, or low oxygen tensions, is a key molecular feature of the tumor microenvironment (TME) that governs the metastatic potential of tumor and stromal cells. Hypoxia develops from an imbalance between oxygen delivery and consumption. Oxygen delivery is impaired in solid tumors due to the abnormal vasculature that develops as a result of an imbalance between pro- and antiangiogenic signals. In addition, oxygen consumption rates are high in proliferating tumor and infiltrating immune cells, leading to hypoxic regions within the TME (8). Hypoxia activates the hypoxia-inducible factor (HIF) signaling pathway in both tumor and stromal cells (9). The prolyl hydroxylase enzymes 1, 2, and 3 (PHD1/2/3) and VHL negatively regulate the HIF signaling pathway under normoxic conditions by cooperatively targeting the hypoxia-inducible transcription factors HIF1 and HIF2 for proteasomal degradation (10). Under hypoxic conditions, HIF1 and HIF2 are stabilized and coordinate the cellular response to hypoxia by activating gene expression programs that facilitate oxygen delivery and cellular adaptation to oxygen deprivation (10). It is well established that HIF1 and HIF2 promote the metastatic potential of tumor cells by activating target genes that stimulate multiple steps within the metastatic cascade including immune evasion, invasion, migration, intravasation/extravasation, and establishment of the premetastatic niche (8). Recent studies have shown that HIF1 and HIF2 can promote prometastatic properties of some tumor–stromal cell populations. Studies with macrophage-specific inactivation of HIF1 or HIF2 have revealed an important role for HIF signaling in mediating the protumorigenic properties of macrophages within multiple tumor models (11, 12). In addition, HIF signaling mediates bidirectional signaling between breast cancer cells and MSCs to promote metastasis (13). In contrast, fibroblast specific inactivation of HIF1 accelerated tumor growth in a murine breast cancer model (14). Further knowledge regarding the role of HIF signaling in mediating tumor–stromal interactions within specific metastatic TME is needed to understand how to best target the hypoxic TME for cancer therapy.

In ovarian cancer, HIF1, HIF2, and hypoxic gene signatures in the primary tumor are associated with poor patient survival and reduced relapse-free survival (15, 16). HIF signaling has been shown to promote cancer stem cell properties, chemoresistance, invasion/migration, immune tolerance, and angiogenesis in ovarian cancer cells *in vitro* (17–21). However, the role of hypoxia and HIF signaling in mediating tumor–stromal interactions in HGSOC are not known.

Here we demonstrate that the omental metastatic microenvironment in HGSOC, a common site of ovarian cancer metastasis, is hypoxic and both tumor cells and mesothelial cells express HIF1 and HIF2. Importantly, hypoxia promotes extracellular collagen fiber deposition by mesothelial cells in a HIF1- and HIF2–dependent manner. In addition, collagen remodeling and HGSOC tumor cell invasion mediated by hypoxic mesothelial and HGSOC cells occurs in an HIF and lysyl oxidase (LOX)-dependent manner, respectively. Pharmacologic inhibition of LOX decreases peritoneal metastasis and collagen crosslinking in the omentum in a murine model of ovarian cancer peritoneal metastases, suggesting that LOX inhibition may be an effective strategy to inhibit HGSOC metastatic progression. These findings reveal a role for mesothelial cells in collagen deposition within the tumor microenvironment and identify the HIF/LOX signaling axis as a druggable therapeutic target to inhibit collagen remodeling and tumor progression in HGSOC peritoneal metastases.

Materials and Methods

Cell culture

HGSOC cancer cell lines OVCAR5 and OVCAR8 were purchased from the National Cancer Institute-Frederick DCTD tumor cell line repository. The LP-9 human peritoneal mesothelial cell line was obtained from Coriell Cell Repositories. Primary human mesothelial cells (PHMC) were derived from omentum of patients with benign disease as described previously (6). All patients who participated in this study provided written informed consent for collection and research use of their materials and use of these samples was approved by the Washington University Institutional Review Board (IRB #201309050). The mouse ID8 ovarian cancer cell line was obtained from Dr. Katherine F. Roby (Department of Anatomy and Cell Biology, University of Kansas Medical Center, Kansas City, KS; ref. 22). All cell lines were authenticated from the original source and were used within 6 months of receipt. In addition, cells were tested upon receipt for viability, cell morphology, and the presence of *Mycoplasma* and viruses (Charles River Laboratories).

HGSOC cell lines OVCAR8 and OVCAR5 and the murine ID8 cell line were cultured in DMEM supplemented with 10% FBS. PHMC and LP-9 were cultured in media containing 45% Ham's F-12, 45% Medium M199, 10% FBS, 0.4 μg/mL hydrocortisone, and 20 ng/mL recombinant EGF. Tumor–mesothelial cell cocultures (OVCAR8+LP9 or OVCAR5+LP9) were cultured in DMEM supplemented with 10% FBS, 1% MEM vitamins, and 1% MEM nonessential amino acids.

Gene signature analysis

The gene expression data for computing the metastatic signature was obtained from GSE30587 (PMID: 24732363). There were 18 Affymetrix Human Gene 1.0 ST arrays corresponding to 9 primary and metastatic ovarian tumors. The arrays were normalized using the standard RMA algorithm. We performed a paired analysis of 9 primary ovarian cancers and their matched metastasis using nonparametric one-sided Wilcoxon signed-rank test. The full list of genes that are significantly increased in metastases can be found in Supplementary Table S1. Previous work (PMID: 2786162) has identified genes that are induced under hypoxic conditions in ovarian cancer cells (GSE66894). Please see ref. 24 and Supplementary Table S6 for the complete list of genes that were hypoxia inducible. There were 3,478 unique genes that were

induced >1.4-fold under hypoxic conditions with FDR-adjusted $P < 0.05$: this constitutes our set of hypoxic genes (23). Overlap between the metastatic and hypoxic genes was assessed using a Fisher exact test. We identified 515 genes with significant overlap (Supplementary Table S2).

siRNA

Transient knockdown of nontargeting control, HIF1, HIF2, HIF1/HIF2, and LOX were achieved in 72 hours by transfection of 100 nmol/L ON-TARGET plus smart pool siRNA using DharmaFECT following manufacturer's protocols (Dharmacon). Cocultures plated at a density of 0.5×10^6 cells per cell type were grown overnight in normoxia followed by transfection of the siRNAs. After 24 hours, the plates were cultured under normoxic and hypoxic conditions in serum-free media for 48 hours and conditioned media were collected.

Conditioned media

The serum-free conditioned media from the coculture plates grown under normoxic and hypoxic conditions were transferred to Amicon Ultra-15 Centrifugal Filter units through a 0.45-μm syringe filter and centrifuged at 4,000 rcf for 30 minutes. The conditioned media collected at the top of the filter was concentrated 10-fold by resuspending in serum-free media.

Collagen gels and confocal microscopy

The conditioned media was utilized to construct an *in vitro* 3D collagen matrix using Corning rat tail collagen I (3.57 mg/mL). Collagen fibril gels (1 mg/mL) were made from Type I rat tail collagen as described previously (24) and were imaged in reflection mode on a Leica SP5 scanning confocal microscope. Collagen fiber amount was calculated using MATLAB. See Supplementary Methods for detailed procedure.

Invasion assay

HGSOC cells were serum starved for 48 hours in normoxia. Matrigel invasion chambers with 8.0-μm pore membranes were primed with 500 μL of the conditioned media overnight in 37°C CO_2 incubator. Serum-starved cancer cells were plated on top of the control inserts or Matrigel invasion inserts and media containing 10% FBS was filled at the bottom of the inserts. Invasion inserts were stained and analyzed 24 hours later. Percent invasion through the Matrigel was normalized against the average number of cells that migrated through the control inserts.

Real-time qPCR

RNA extraction, reverse transcription, and real-time PCR analysis was performed as described previously (25). Relative mRNA expression levels of the target genes were determined by normalizing against the corresponding mRNA levels of 18S. The sequences of human primer sets are summarized in Supplementary Table S3.

Western blotting

Protein lysates from cells cultured in normoxia and hypoxia for 48 hours were harvested as described previously (26). Antibodies HIF1, HIF2, P4HA1 (Novus Biologicals), COL1A1, LOX, P4HA3 (Abcam), P4HA2, PLOD2 (Abclonal), PLOD1 (Biorbyt), PLOD3 (Invitrogen), and HSP-70 (Sigma) were used. Horseradish peroxidase–conjugated secondary antibodies were probed for 1 hour at room temperature.

IHC

Paraffin-embedded tissue sections were deparaffinized and stained according to previously published protocols (27). Primary antibodies HIF1 (anti-rabbit A300-286A; 1:100; Bethyl Laboratories), HIF2 (anti-rabbit NB100-122; 1:100; Novus Biologicals), LOX (anti-rabbit ab174316; 1:500; Abcam), and PIMO (anti-rabbit; 1:100; Hypoxyprobe) were used.

Immunofluorescence

Staining was performed following the protocol mentioned above. See detailed protocol in Supplementary Methods.

Picrosirius red staining

Collagen was stained by Picrosirius red as described in http://www.ihcworld.com/_protocols/special_stains/sirius_red.htm.

Human normal and tumor omentum tissues

Human normal and tumor omentum were obtained from patients under IRB approval #201709191 in accordance with recognized ethical guidelines per the U.S. Common Rule. Patients were treated at Washington University in St. Louis (St. Louis, MO) and written informed consent was obtained for tissue banking. Ovarian cancer metastatic tissue array containing 40 cores of metastatic cases in duplicates was obtained from US Biomax.

Peritoneal xenografts

Eight-week-old female NSG mice were randomized into saline or BAPN treatment groups ($n = 8$). BAPN (100 mg/kg) or saline was administered intraperitoneally daily. OVCAR8 cells (1×10^6) were injected intraperitoneally 3 days after BAPN pretreatment. After 5 weeks of BAPN treatment, the animals were euthanized and metastatic burden was determined.

For the murine ID8 model, 5×10^6 ID8 cells were injected intraperitoneally into 8-week-old female C57BL/6 mice. Twenty-eight days after tumor injection, mice were injected intraperitoneally with 75 mg/kg of pimonidazole. Ninety minutes later, mice were euthanized and tissues were collected and fixed in 10% formalin.

All procedures for use of animals and their care were approved by the Institutional Animal Care and Use Committee of Stanford University in accordance with the institutional and NIH guidelines.

Second harmonic generation microscopy

Forty-micron–thick sections were sectioned using a vibratome (Leica) and the sections were imaged floating in PBS at ×100 magnification using SP8 DIVE FALCON SHG (second harmonic generation) microscope (Leica). Tile scanning and Z-stacks were performed using Leica software and the images are presented as extended depth of field merge of the Z-stacks. Collagen fiber amount in the tumor-bearing omentum was calculated for three regions of interest (ROI) per image.

Statistical analysis

Statistical significance was computed using GraphPad Prism. Two-way ANOVA and two-tailed unpaired *t* tests were performed. $P < 0.05$ (*) was considered statistically significant.

Natarajan et al.

Results

HIF signaling is active and associated with hypoxia in the ovarian cancer metastatic microenvironment

To determine whether hypoxic signaling influences HGSOC tumor–mesothelial interactions in the metastatic microenvironment, we first examined whether hypoxic signaling is active within the human HGSOC omental metastatic microenvironment. For this purpose, we examined whether hypoxic gene signatures are expressed in HGSOC metastatic gene signatures. Retrospective analysis of primary and matched metastases in a cohort of patients with HGSOC who were chemotherapy naïve ($n = 9$) showed that 2,431 genes were differentially over-expressed in metastatic tumors compared with matched primary tumors (Fig. 1A, $P < 0.05$, Supplementary Table S1; ref. 28). Previous analysis of hypoxic gene signatures in human ovarian cancer cells revealed that 3,478 genes were upregulated more than 1.4-fold by hypoxia compared with normoxia (Fig. 1A; ref. 23). We identified 515 genes that overlapped between the hypoxic gene signature and the metastatic gene

signature derived from patients with HGSOC (Fig. 1A, P of overlap = 4.764e-09; Supplementary Table S2). These findings suggest a link between hypoxic signaling and the HGSOC metastatic microenvironment. Functional gene enrichment analysis of the 515 genes that overlap between hypoxic and HGSOC metastatic gene signatures using the Search Tool for the Retrieval of Interacting Genes/Proteins (STRING) database revealed that there were multiple genes involved in extracellular matrix organization, collagen catabolic processes, extracellular matrix disassembly, and collagen fibril organization (Fig. 1A).

We next performed IHC analysis of the hypoxia-inducible transcription factors HIF1 and HIF2 in benign human omentum ($n = 3$) and HGSOC omental metastases ($n = 40$) to determine whether HIF1 and HIF2 are expressed within HGSOC omental metastases. We observed basal levels of HIF1 and HIF2 staining within benign human omentum that were significantly increased in HGSOC omental metastatic lesions (Fig. 1B and C). HIF1 and HIF2 staining within HGSOC omental metastases was observed
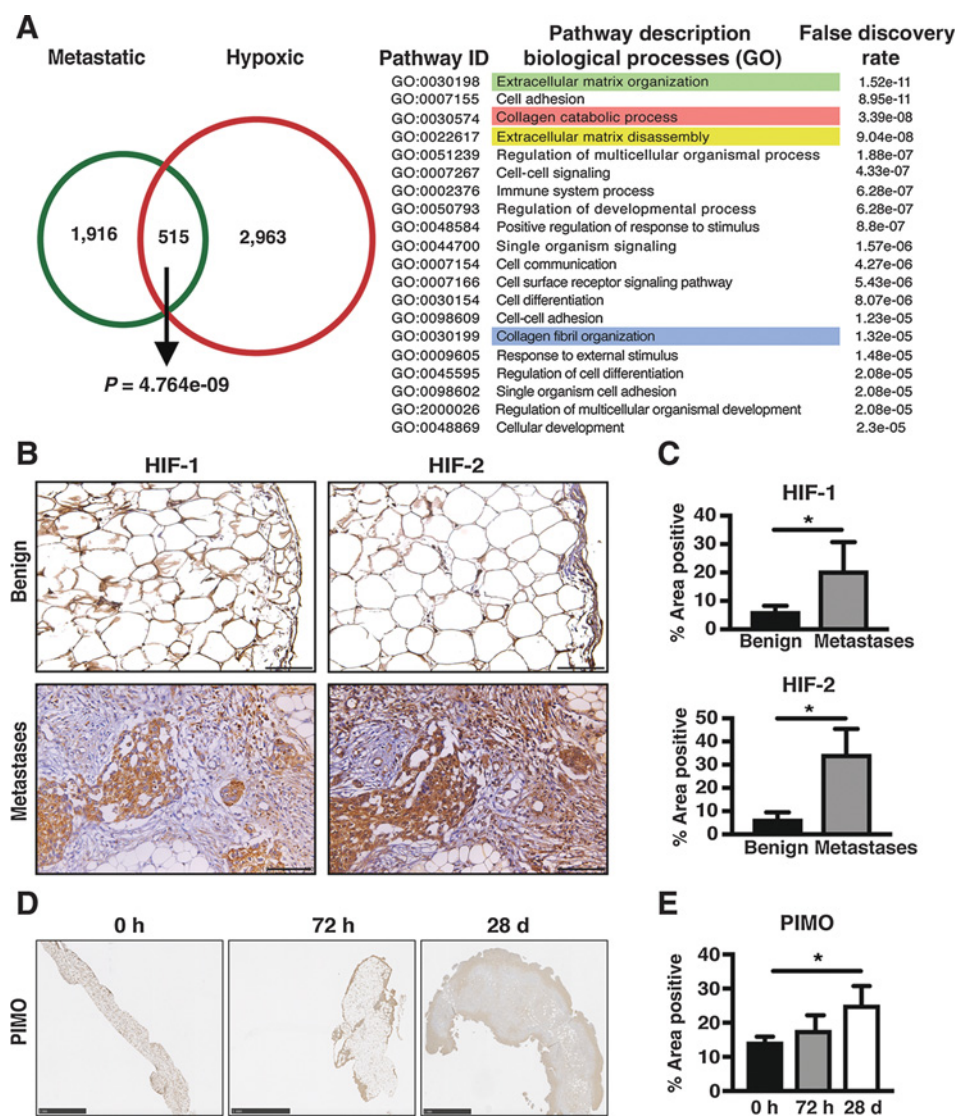

Figure 1.

The metastatic microenvironment in ovarian cancer is hypoxic and expresses HIF1 and HIF2. **A,** Computational analysis showing overlapping gene signatures of HGSOC metastases with hypoxic gene signatures. Metastatic gene signatures were derived from comparison of matched primary ovarian and omental metastatic tumors ($n = 9$). Hypoxic gene signatures were derived from comparing normoxic and hypoxic gene expression in human ovarian cancer cells. Table shows the top 20 functional biological processes enriched among the overlapping gene signatures (GO enrichment pathway) derived using the STRING database. The pathways associated with collagen biogenesis and remodeling are highlighted. **B,** IHC staining of benign human omentum ($n = 3$) and HGSOC omental metastases ($n = 40$) for hypoxia-inducible factors HIF1 and HIF2. Scale bars, 100 μm. **C,** Quantification of the percentage area positive for HIF1 and HIF2 in the benign omentum and omental metastases. **D,** PIMO staining of naïve mouse (0 hours) and murine omental metastases formed at 72 hours (h) and 28 days (d) upon intraperitoneal injections of ID8 cells ($n = 3$ per group). Scale bar, 1 mm. **E,** Quantification of the percentage area positive for PIMO in the murine naïve and ID8 tumor–bearing omentum. Error bars, SD of the mean. *, $P < 0.05$.

in both tumor and stromal cells (Fig. 1B). We next examined whether the stabilization of HIF1 and HIF2 in ovarian omental metastases was associated with a hypoxic microenvironment. The ID8 murine model of ovarian metastasis was used to directly examine the hypoxic status of the omental metastatic microenvironment (22). We used the hypoxic probe pimonidazole (PIMO) as a hypoxic cell marker to profile regions of hypoxia in the omentum of naïve and ID8 ovarian tumor–bearing C57BL/6 mice. At oxygen tensions below 1%, pimonidazole forms protein adducts that can be efficiently detected by IHC analysis (29). As a positive control, pimonidazole adducts were readily detectable in hypoxic regions of the central vein of the liver (Supplementary Fig. S1A; ref. 30). In the omentum, pimonidazole adducts were detected at basal levels throughout the naïve omentum and increased in the tissue during metastatic tumor progression from 72 hours to 28 days after peritoneal tumor cell inoculation (Fig. 1D and E; Supplementary Fig. S1A). Pimonidazole staining within the total tumor-bearing omentum at late stages (28 days) of disease increased (Fig. 1D). Interestingly, the pattern of PIMO

staining was increased near the periphery of the omental metastatic tissue compared with the naïve omentum (Fig. 1D). Regions of pimonidazole staining in the ID8 tumor-bearing omentum overlapped with regions of HIF1 and HIF2 expression (Supplementary Fig. S1B). Our findings indicate that the metastatic microenvironment in ovarian omental metastases is hypoxic and expresses HIF1 and HIF2.

As mesothelial cells are a key cellular component of the HGSOC metastatic microenvironment, we next sought to determine whether mesothelial cells express HIF1 and/or HIF2. Immuno-fluorescence analysis of HIF1, HIF2, and the mesothelial cell marker calretinin in HGSOC omental metastases demonstrated that mesothelial cells express HIF1 and HIF2 in HGSOC omental metastases (Fig. 2A; ref. 31). Western blot analysis for HIF1 and HIF2 confirmed that both PHMCs isolated from omentum and the LP-9 peritoneal mesothelial cell line derived from ascites fluid from a patient with HGSOC express HIF1 and HIF2 under hypoxic conditions (Fig. 2B; ref. 32). Moreover, the HIF1 and HIF2 targets including PGK1 and VEGFA were induced upon hypoxia
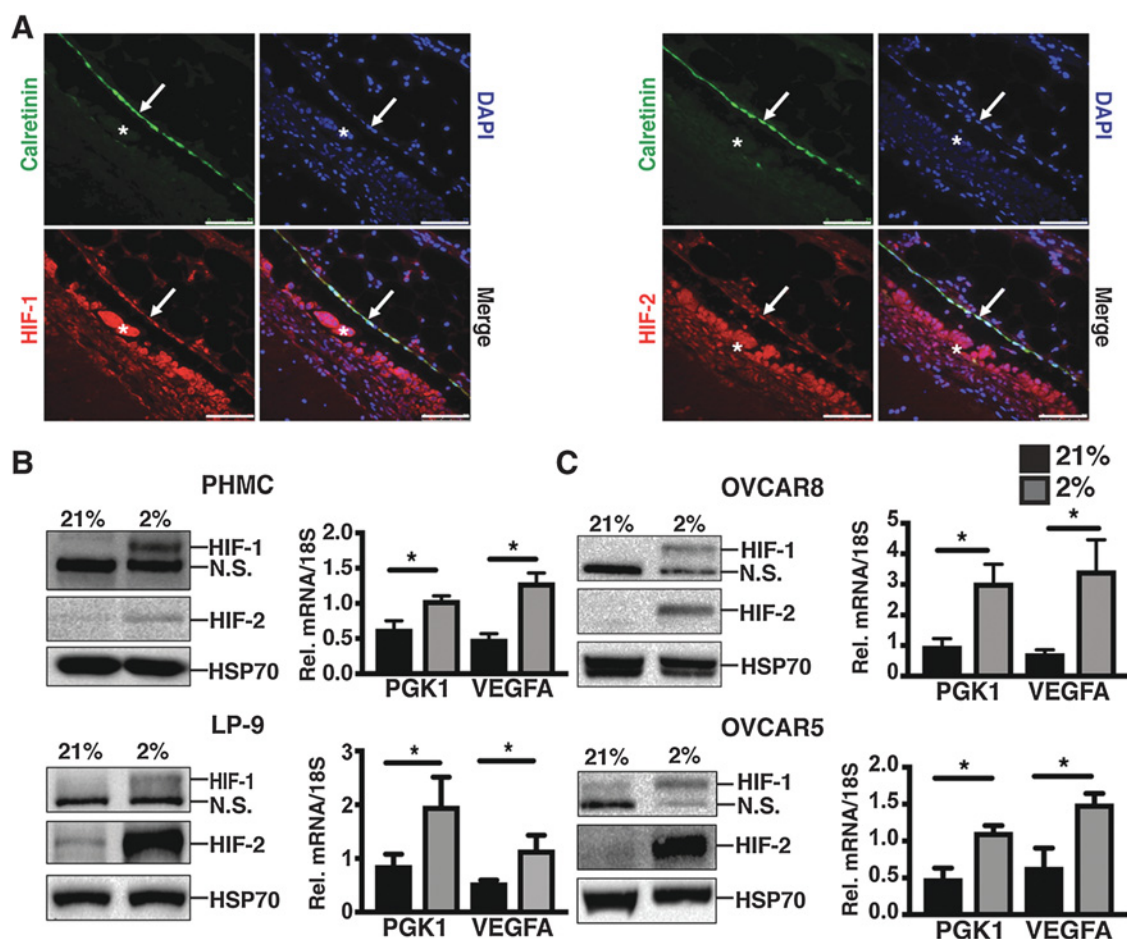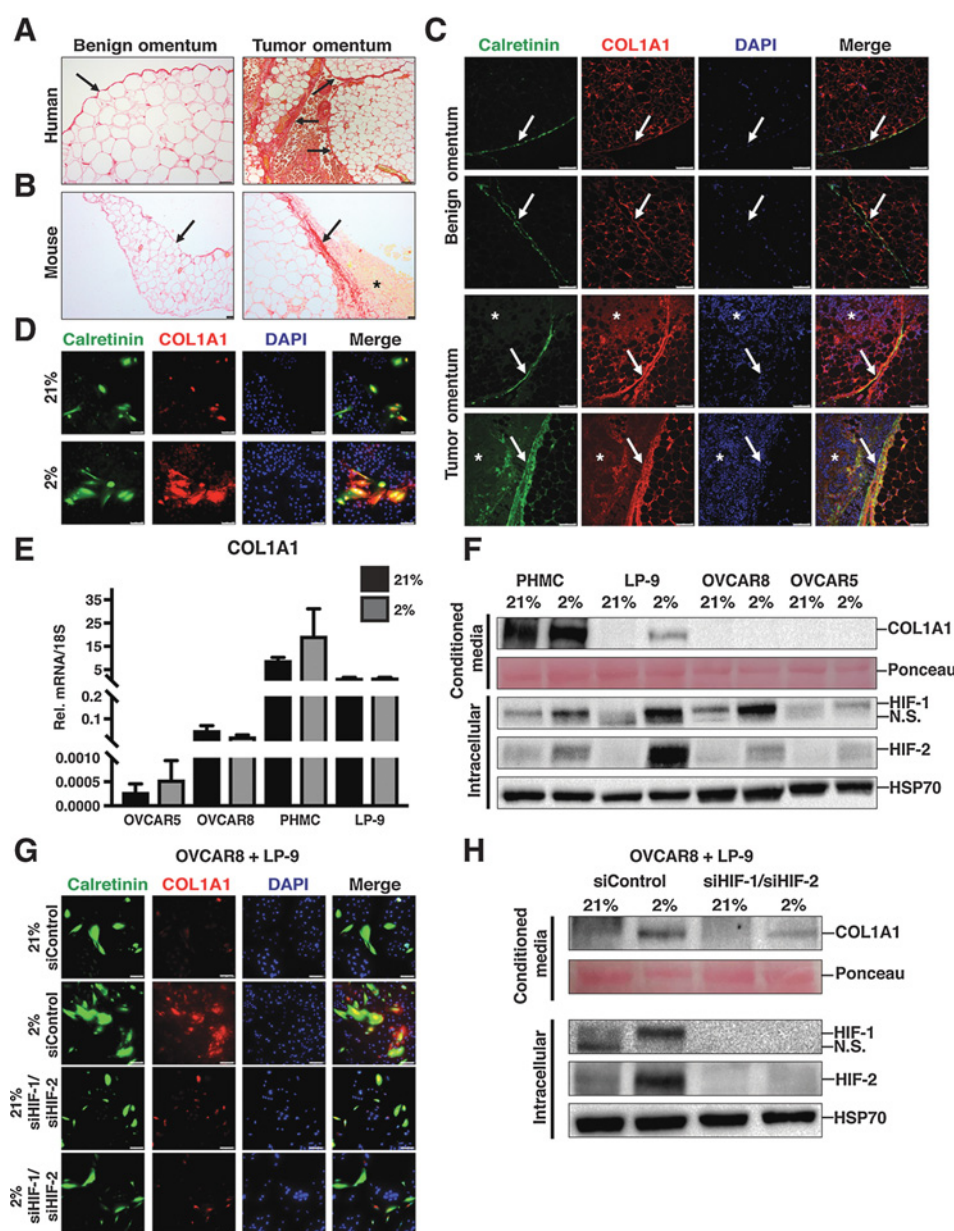

Figure 2.
Tumor and mesothelial cells in the HGSOC metastatic microenvironment express HIF1 and HIF2. **A,** Immunofluorescent staining showing colocalization of mesothelial cell marker calretinin with HIF1 and HIF2 in patient HGSOC omentum. Arrows, mesothelial lining of the omentum. Asterisks, tumor deposits. Pictures are representative of three patient samples. Calretinin, green; HIF1 and HIF2, red; nucleus, blue. Scale bar, 75 μm. **B** and **C,** Western blot analysis of HIF1 and HIF2 expression levels (left) and real-time quantitative PCR analysis (right) of the mRNA expression levels of the HIF targets PGK1 and VEGFA in the mesothelial cells (PHMC and LP-9) and the HGSOC cells (OVCAR8 and OVCAR5) exposed to normoxia (21%) and hypoxia (2%; $n = 3$). HSP-70 was used as the protein-loading control. Error bars, SD of the mean. *, $P < 0.05$.

Natarajan et al.

Figure 3.
Hypoxia promotes the secretion of type I collagen by mesothelial cells through HIF1 and HIF2. **A,** Picrosirius red staining showing collagen deposition in the benign and metastatic tumor omentum in human (pictures are representative of three benign and 40 tumor omentum; scale bar, 100 μm). **B,** Representative pictures of three naïve and three ID8 tumor–bearing omentum. Scale bar, 25 μm. **C,** Immunofluorescent staining of two different patient tissue sections of benign and HGSOC omentum for calretinin and type I collagen COL1A1. Calretinin, green; COL1A1, red; DAPI, blue. Scale bar, 100 μm. Arrows, mesothelial lining of the omentum. Asterisks, tumor deposits. **D,** Immunofluorescent staining of cocultures of OVCAR8 and LP-9 cells cultured under normoxic (21%) and hypoxic (2%) conditions. Calretinin, green; COL1A1, red; DAPI, blue. Scale bar, 100 μm. **E,** Real-time qPCR analysis of mRNA expression levels of COL1A1 in HGSOC cells (OVCAR5, OVCAR8) and mesothelial cells (PHMC, LP-9) under normoxic (21%) and hypoxic (2%) conditions ($n = 3$). Error bars, SD of the mean. **F,** Western blot analysis of conditioned media (top) for COL1A1 and intracellular extracts (bottom) for HIF1 and HIF2 to confirm hypoxic induction of HIF1 and HIF2 from mesothelial cells (PHMC and LP-9) and HGSOC cells (OVCAR8 and OVCAR5). **G,** Immunofluorescent staining of cocultures of OVCAR8 and LP-9 cells cultured under normoxic (21%) and hypoxic (2%) conditions and treated with siRNA against HIF1 and HIF2 or siRNA targeting the scrambled control. Calretinin, green; COL1A1, red; DAPI, blue. Scale bar, 100 μm. Immunofluorescent images are representative of three biologic and three technical replicates. **H,** Western blot analysis of the conditioned media (top) and intracellular extracts (bottom) from cocultures of OVCAR8 and LP-9 treated with scrambled siControl or siRNA targeting HIF1 and HIF2. Ponceau stain shows loading control of protein lysates from the conditioned media, and HSP70 shows loading control of intracellular protein lysates.

treatment (Fig. 2B; ref. 33). In addition to mesothelial cells, HGSOC cells express HIF1 and HIF2 upon hypoxic treatment *in vitro* and in HGSOC metastases (Fig. 2A and C). These findings demonstrate that HIF1 and HIF2 are expressed in both mesothelial and tumor cells within the HGSOC tumor–mesothelial microenvironment and cell lines.

Mesothelial cells express collagen type I and induce collagen secretion in a HIF-dependent manner

We next sought to investigate the functional role of hypoxia and HIF signaling in regulating mesothelial and HGSOC tumor functions. Our analysis of metastatic and hypoxic gene expression profiles in Fig. 1A suggests that hypoxic signaling may influence collagen matrix organization in HGSOC metastases. Enhanced collagen type I deposition has recently been associated with increased tumor burden in HGSOC metastases (34). In addition, collagen remodeling into long collagen bundles is correlated with tumor burden in HGSOC metastases (34). Moreover, collagen remodeling signatures are associated with poor patient survival in HGSOC (35). However, the cellular and molecular mechanisms that drive collagen deposition and remodeling in the HGSOC metastatic microenvironment are not known.

Here we investigated whether mesothelial and/or HGSOC tumor cells contribute to enhanced collagen deposition and remodeling in HGSOC metastases. We first analyzed benign human and HGSOC tumor-bearing omentum for collagen deposition by Picrosirius red staining (36). Consistent with previous reports, we observed that collagen type I deposition increased in the human tumor-bearing omentum compared with the benign omentum (Fig. 3A; ref. 34). Moreover, we

observed increased collagen type I deposition by Picrosirius red staining within the omentum of C57BL/6 mice bearing ID8 ovarian tumors compared with naïve omentum (Fig. 3B). Picro Sirius red staining within the human and mouse tumor-bearing omentum showed increased collagen fiber deposition within regions where the tumor was adjacent to the omentum surface (Fig. 3A and B). To determine whether there is enhanced COL1A1 expression in mesothelial cells of HGSOC compared with mesothelial cells in naïve omentum, we performed immunofluorescence analysis for calretinin-positive mesothelial cells and collagen type I (COL1A1) within human benign and HGSOC omentum. Calretinin-positive mesothelial cells produced more COL1A1 fibers in HGSOC omentum compared with the benign human omentum, suggesting that mesothelial cells contribute to enhanced collagen deposition within HGSOC omental metastases (Fig. 3C). Immunofluorescence analysis of COL1A1 in normoxic and hypoxic HGSOC tumor–mesothelial cell cocultures confirmed that calretinin-positive mesothelial cells, but not calretinin-negative tumor cells, produce COL1A1 *in vitro* (Fig. 3D). Interestingly, most of the type I collagen was intracellular in mesothelial cells under normoxic conditions, whereas under hypoxic conditions the type I collagen produced by mesothelial cells was deposited in the extracellular space into long fibers (Fig. 3D). We next compared the relative expression of COL1A1 mRNA in human mesothelial cells (PHMC and LP-9) and HGSOC (OVCAR5 and OVCAR8) cells under normoxic and hypoxic conditions. We observed very low, almost undetectable, levels of COL1A1 in OVCAR5 and OVCAR8 cells under normoxic and hypoxic conditions (Fig. 3E). In contrast, we observed robust expression of COL1A1 in human PHMC and LP-9 cells (Fig. 3E). COL1A1
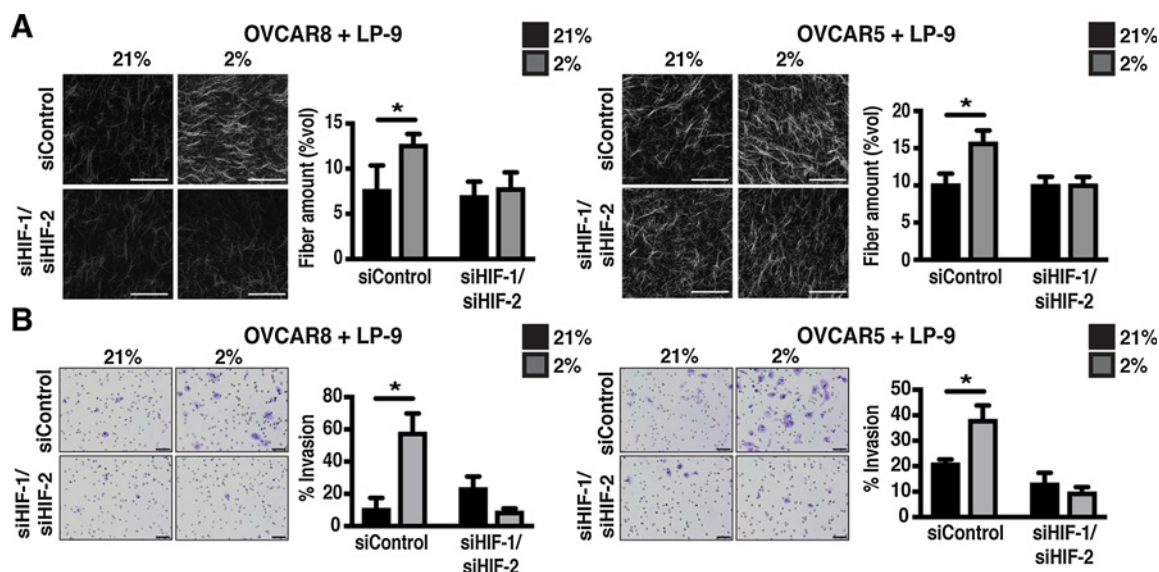

Figure 4.
Hypoxia promotes collagen remodeling and invasion mediated by HGSOC tumor–mesothelial cocultures in a HIF1– and HIF2–dependent manner. **A,** Representative confocal images of collagen fibers from 3D collagen gels constructed using conditioned media from cocultures of OVCAR8 + LP-9 and OVCAR5 + LP-9 exposed to normoxia (21%) and hypoxia (2%) that were treated either with siRNA targeting HIF1 and HIF2 or siRNA targeting the scrambled control. Graphs show the corresponding quantification of the percentage volume of fiber amounts. Scale bar, 75 μm; $n = 3$. **B,** Matrigel invasion assays of OVCAR8 or OVCAR5 cells through Matrigel inserts primed with conditioned media from cocultures of OVCAR8 + LP-9 and OVCAR5 + LP-9 exposed to normoxia (21%) and hypoxia (2%) that were treated either with siRNA targeting HIF1 and HIF2 or siControl. Scale bar, 75 μm; $n = 3$. Graphs represent the normalized percentage of invading cells per field. Error bars, SD of the mean. *, $P < 0.05$.

Natarajan et al.
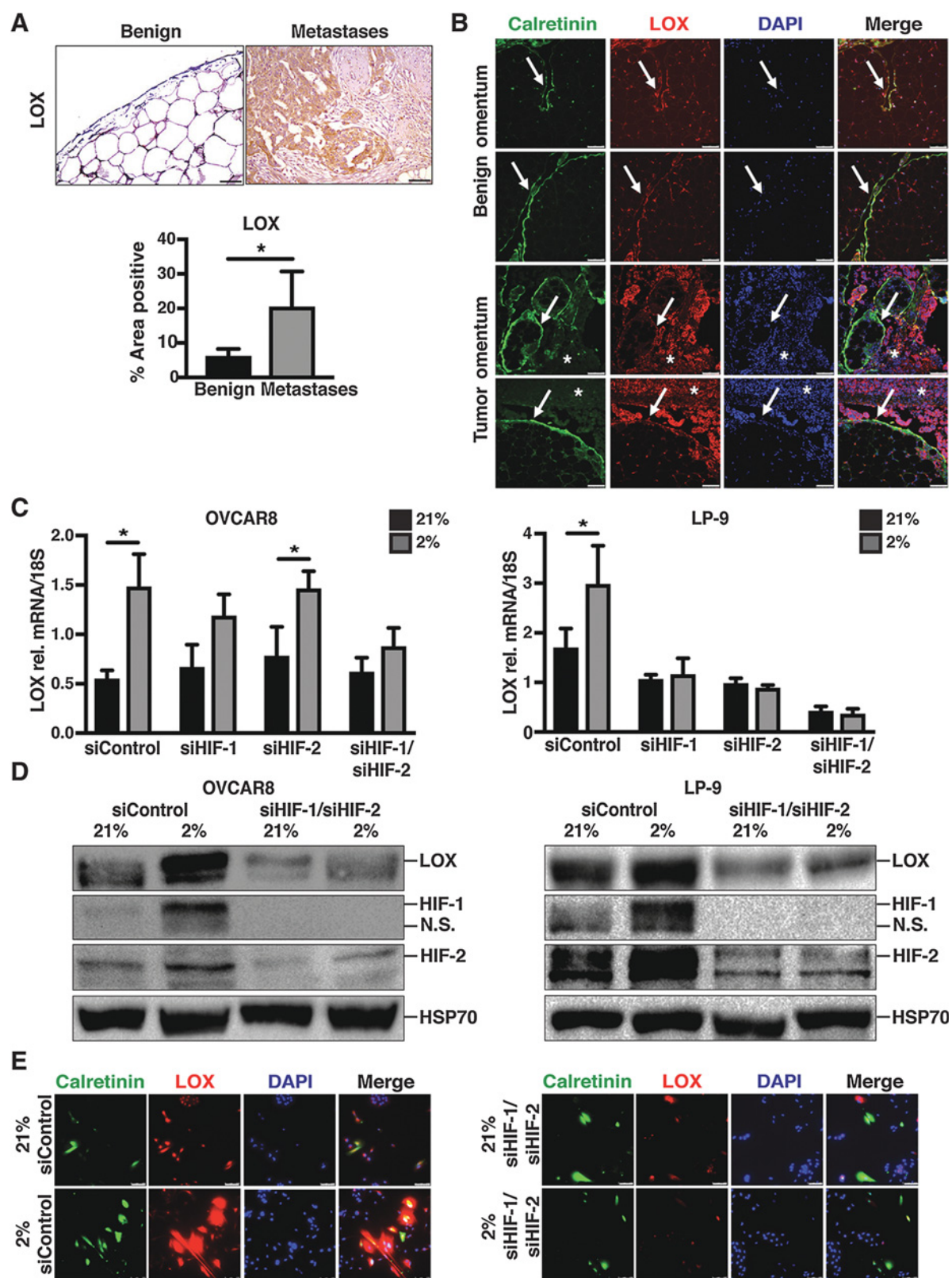
mRNA expression was not changed under hypoxic conditions compared with normoxic conditions within human mesothelial cells (Fig. 3E). Western blot analysis of conditioned media collected from normoxic and hypoxic mesothelial cell (LP-9, PHMC) or HGSOC cancer (OVCAR8, OVCAR5) cultures confirmed that mesothelial cells, but not HGSOC cells, secrete type I collagen (Fig. 3F). Interestingly, COL1A1 secretion in mesothelial cells was enhanced under hypoxic conditions. Collectively, our findings indicate that mesothelial cells contribute to collagen type I deposition in HGSOC and collagen type I secretion by mesothelial cells is enhanced under hypoxic conditions.

The molecular mechanisms driving collagen synthesis and the formation of covalent cross-linked collagen fibrils within the extracellular matrix are complex (37). Previous studies have demonstrated that hypoxia and HIF signaling can promote the synthesis and stability of fibril-forming collagen through the upregulation of the intracellular enzymes including collagen prolyl 4-hydroxylases (P4HA1 and P4HA2) and lysyl hydroxylases (PLOD1 and PLOD2; refs. 38–42). Strikingly, we found a number of these factors in the overlapping hypoxic and HGSOC metastatic gene signatures (pathways highlighted in Fig. 1A). STRING network analysis of the genes within these pathways revealed protein–protein interactions among multiple collagen family members as well as enzymes involved in fibrillar collagen synthesis and remodeling (Supplementary Fig. S2A). Therefore, we examined the relative expression of these factors within human mesothelial (PHMC, LP-9) cells under normoxic and hypoxic conditions. While the expression of COL1A1 was not increased under hypoxia, the expression of intracellular enzymes responsible for collagen biogenesis (P4HA1, P4HA2, P4HA3) and their mechanical stability (PLOD1 and PLOD2) were significantly induced at the mRNA level by hypoxia compared with normoxia within mesothelial cells (Fig. 3E; Supplementary Fig. S2B and S2C). Western blot analysis confirmed a hypoxic induction at the protein level of P4HA1 and P4HA3 in PHMC as well as PLOD2 in both PHMC and LP9 cells in hypoxic mesothelial cells compared with normoxic mesothelial cells (Supplementary Fig. S2D and S2E). These findings demonstrate that the hypoxic induction of extracellular collagen deposition by human mesothelial cells is associated with the upregulation of collagen biogenesis and stability enzymes.

To determine whether hypoxia promotes collagen deposition by mesothelial cells in an HIF1 and HIF2–dependent manner, we treated human HGSOC and peritoneal mesothelial cells (OVCAR8 and LP-9) with siControl or siHIF1 and siHIF2 smart pools and cocultured the cells under normoxic or hypoxic conditions for 48 hours. Immunofluorescence microscopy of the siControl cocultures confirmed our previous findings that

mesothelial cells are the source of type I collagen and collagen deposition by mesothelial cells is increased under hypoxic conditions (Fig. 3G). In comparison with the siControl cocultures, the siHIF1/HIF2 cocultures had reduced type I collagen fibers under hypoxic conditions (Fig. 3G). Western blot analysis of conditioned media collected from normoxic and hypoxic HGSOC tumor and mesothelial cell cocultures confirmed that the hypoxic secretion of collagen type I by mesothelial cells in HGSOC tumor–mesothelial cocultures occurs in a HIF1 and HIF2–dependent manner (Fig. 3H). These findings suggest that hypoxic signaling mediated by HIF1 and HIF2 contributes to enhanced collagen deposition by mesothelial cells.

Tumor–mesothelial cocultures enhance extracellular collagen type I remodeling in a HIF-dependent manner

Once collagen is secreted into the extracellular space, collagen fiber formation is mediated by the LOX family of collagen cross-linking enzymes. In breast cancer, collagen crosslinking and fiber formation mediated by LOX family members promotes tumor cell invasion and metastasis (43, 44). Collagen fibril organization pathways were enriched in the overlapping metastatic and hypoxic HGSOC gene expression analysis performed in Fig. 1. Therefore, we examined the ability of conditioned media collected from normoxic and hypoxic HGSOC tumor–mesothelial cocultures to modify collagen crosslinking. Type I collagen was incubated with conditioned media from OVCAR5 or OVCAR8 and LP-9 cocultures that were treated with siControl or siHIF1 and siHIF2 smart pools and incubated under normoxic or hypoxic conditions. Reflection confocal microscopy showed that the conditioned media from hypoxic cocultures significantly increased the percentage of collagen type I fibers in a HIF1 and HIF2–dependent manner (Fig. 4A).

We next hypothesized that HIF-mediated collagen remodeling mediated by secreted factors within HGSOC tumor–mesothelial cocultures may promote HGSOC tumor invasion. We examined whether the conditioned media from normoxic or hypoxic tumor–mesothelial cocultures enhanced HGSOC invasion in a HIF-dependent manner. HGSOC tumor cell invasion through Matrigel inserts primed with conditioned media from siControl or siHIF1/siHIF2–treated tumor (OVCAR8 or OVCAR5)-mesothelial (LP-9) cocultures revealed that hypoxic conditioned media facilitated the invasion of OVCAR5 and OVCAR8 HGSOC cells in an HIF1- and HIF2–dependent manner (Fig. 4B). These findings demonstrate that hypoxic signaling in tumor–mesothelial cocultures results in the production of secreted factors that promote collagen fiber formation and tumor cell invasion in a HIF1- and HIF2–dependent manner.

Figure 5.
Hypoxia upregulates LOX in both tumor and mesothelial cells in a HIF-dependent manner. **A,** IHC staining of benign human omentum ($n = 3$) and HGSOC omental metastases ($n = 40$) for LOX. Scale bars, 100 μm. Graph shows the quantification of the percentage area positive for LOX in the benign and metastatic human omentum. **B,** Immunofluorescent staining of two different patient tissue sections of benign and tumor omentum for calretinin and LOX. Calretinin, green; LOX, red; DAPI, blue. Scale bar, 100 μm. Arrows, mesothelial lining of the omentum. Asterisks, tumor deposits. **C,** Real-time quantitative PCR analysis of LOX expression in OVCAR8 and LP-9 cells exposed to normoxic (21%) and hypoxic (2%) culture conditions that were treated with siRNA pools against control, HIF1 and HIF2 targeting sequences ($n = 3$). Error bars, SD of the mean. *, $P < 0.05$. **D,** Western blot analysis of LOX expression in OVCAR8 and LP-9 cells. Western blots also confirm the downregulation of HIF1 and HIF2 in both the models (OVCAR8 and LP-9) upon treatment with siHIF1/siHIF2. HSP-70 was used as the protein-loading control. **E,** Immunofluorescent staining of cocultures of OVCAR8 and LP-9 cells cultured under normoxic (21%) and hypoxic (2%) conditions that were treated with siRNA pools targeting HIF1 and HIF2 or scrambled control. Images are representative of three biologic and three technical replicates. Calretinin, green; LOX, red; DAPI, blue. Scale bar, 100 μm.

Natarajan et al.

Hypoxic mesothelial and HGSOC tumor cells upregulate LOX in a HIF-dependent manner to promote collagen remodeling and tumor invasion

We next sought to identify druggable downstream targets of HIF1 and HIF2 within the secreted tumor–mesothelial cocultures that promote HGSOC collagen fiber formation, tumor invasion, and metastasis. Analysis of the overlapping metastatic and hypoxic genes identified multiple LOX family members known to mediate collagen fiber formation (Supplementary Fig. S2A). LOX is a secreted amine oxidase and a druggable target that mediates the covalent crosslinking of collagen and elastin within the extracellular matrix (45). Recent studies have shown that LOX expression is associated with ovarian cancer metastasis, chemoresistance, and poor survival (35, 46, 47). However, the role of LOX in mediating collagen remodeling and tumor progression within metastatic sites in ovarian cancer is not known. We found that LOX is highly expressed within HGSOC omental metastases compared with benign human omentum (Fig. 5A). Moreover, immunofluorescent staining for LOX and calretinin in benign and HGSOC metastatic omentum revealed that LOX is expressed by both tumor cells and mesothelial cells (Fig. 5B). To determine whether LOX is a HIF1 and HIF2 target in HGSOC tumor and/or mesothelial cells, we exposed HGSOC and human mesothelial cells to normoxic or hypoxic conditions. LOX was significantly induced at the mRNA and protein level in both hypoxic HGSOC (OVCAR5, OVCAR8) and human mesothelial cells (PHMC, LP-9) in an HIF1- and HIF2–dependent manner (Fig. 5C and D; Supplementary Fig. S3A–S3D). We further confirmed the HIF-dependent hypoxic induction of LOX in cocultures of OVCAR8 and LP-9 by immunofluorescent staining for LOX. Costaining of LOX with the mesothelial cell marker calretinin in the OVCAR8 + LP-9 cocultures revealed LOX expression in both calretinin-positive mesothelial cells and calretinin-negative tumor cells (Fig. 5E). LOX expression in these cells was induced upon hypoxic conditions in a HIF-dependent manner (Fig. 5E). These findings demonstrate that HIF1 and HIF2 are required for the hypoxic upregulation of LOX in the HGSOC tumor and mesothelial cells.

To determine whether LOX is an important factor contributing to hypoxia-induced collagen fiber remodeling and invasion within HGSOC tumor and/or mesothelial cells, we first investigated whether genetic inactivation of LOX is sufficient to reduce collagen type I fiber formation under normoxic and hypoxic conditions in HGSOC tumor–mesothelial cocultures. Genetic inhibition of LOX using siRNA smart pools in HGSOC tumor (OVCAR5 or OVCAR8) and mesothelial cell (LP-9) cocultures significantly inhibited the ability of conditioned media to promote type I collagen fiber formation under hypoxic conditions (Fig. 6A; Supplementary Fig. S4A and S4B). We next investigated whether single cultures of HGSOC tumor (OVCAR8) or mesothelial (LP-9) cells enhance collagen remodeling under hypoxic conditions. Conditioned media from both HGSOC tumor (OVCAR8) or mesothelial (LP-9) cells independently increased the percentage of collagen type I fibers under hypoxic conditions compared with normoxic conditions. Similar to the HGSOC tumor–mesothelial cocultures, the hypoxic induction of collagen type I fiber formation occurred in a LOX-dependent manner within HGSOC and mesothelial cell single cultures (Fig. 6A; Supplementary Fig. S4A). These findings are consistent with data in Fig. 5C–E demonstrating that both HGSOC tumor and mesothelial cells increase LOX expression under hypoxic conditions. Given that collagen
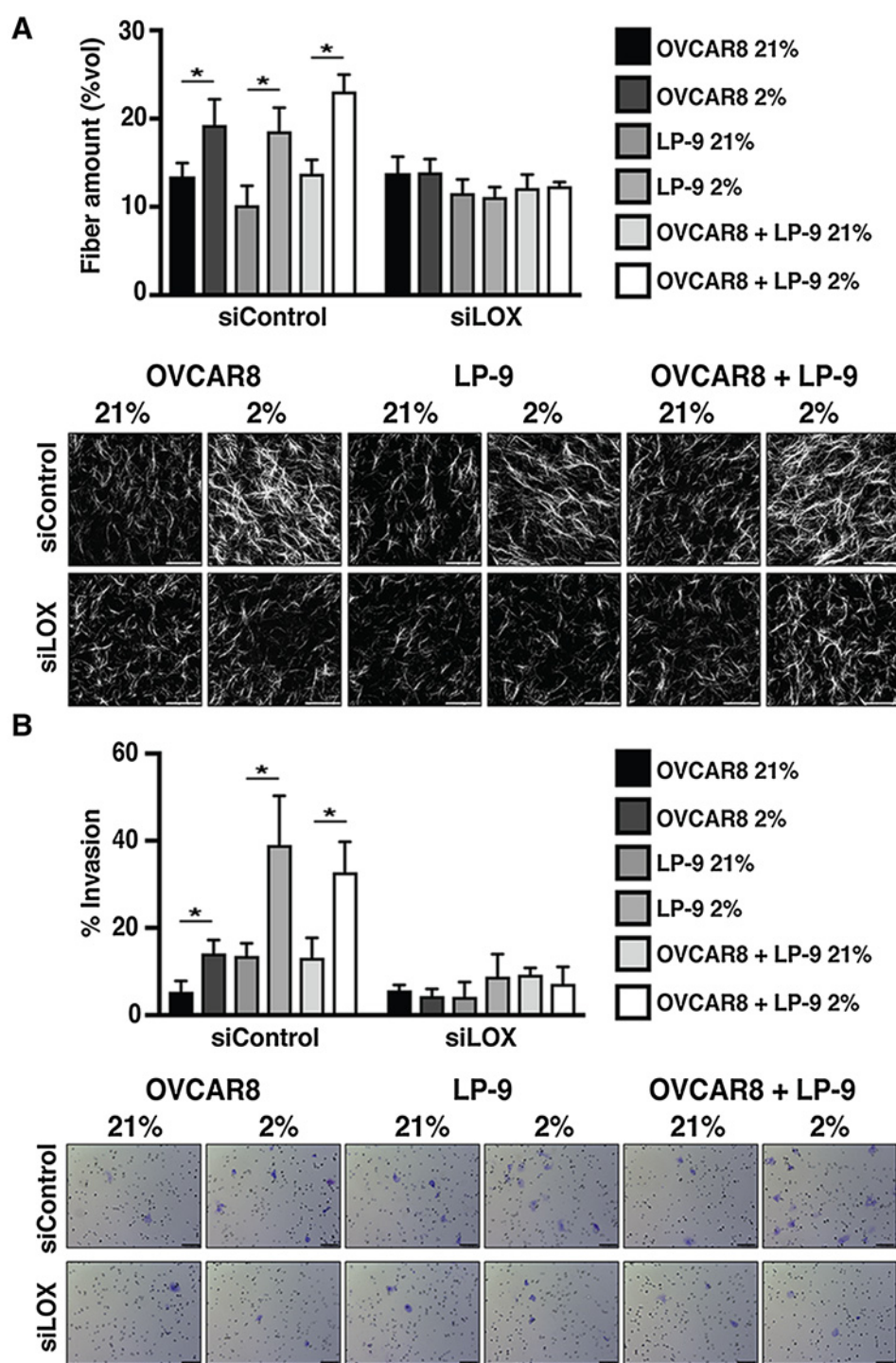
fiber formation can promote tumor cell invasion, we next examined whether conditioned media from normoxic or hypoxic HGSOC tumor, mesothelial, or tumor–mesothelial cocultures are sufficient to precondition Matrigel substrate to facilitate HGSOC tumor cell invasion in a LOX-dependent manner. Genetic inactivation of LOX significantly reduced the ability of conditioned media collected from hypoxic HGSOC, mesothelial and tumor–mesothelial cocultures to promote HGSOC invasion compared with the HGSOC invasion mediated by conditioned media from the corresponding siControl cultures (Fig. 6B; Supplementary Fig. S4C). These findings demonstrate that LOX is an important secreted factor driving collagen remodeling and tumor invasion mediated by HGSOC tumor and mesothelial cells.

Therapeutic inhibition of LOX inhibits metastatic ovarian cancer progression *in vivo*

The findings above identify a role for LOX in facilitating collagen remodeling and tumor invasion mediated by HGSOC tumor and mesothelial cells, raising the intriguing possibility that therapeutic inhibition of LOX may be an effective strategy for the treatment of metastatic HGSOC. Several classes of LOX inhibitors have been developed and have shown efficacy in preclinical models of metastasis including the small-molecule inhibitor of LOX enzymatic activity β-aminopropionitrile (BAPN; ref. 45). We first examined whether pharmacologic inhibition of LOX using BAPN is sufficient to inhibit collagen remodeling and HGSOC tumor cell invasion mediated by HGSOC tumor–mesothelial cell cocultures *in vitro*. BAPN treatment of HGSOC tumor (OVCAR5 or OVCAR8) and mesothelial (LP-9) cocultures significantly reduced type I collagen fiber formation induced by conditioned media collected from hypoxic cocultures (Fig. 7A). Moreover, BAPN treatment significantly reduced the ability of HGSOC (OVCAR5 or OVCAR8) and LP-9 coculture conditioned media to stimulate HGSOC cell invasion through preconditioned Matrigel substrates (Fig. 7B). To determine the efficacy of BAPN in metastatic HGSOC, we treated mice harboring OVCAR8 human HGSOC tumors with BAPN (100 mg/kg) or saline daily for 5 weeks. BAPN treatment resulted in a significant reduction in the number of peritoneal tumor nodules and total tumor weight compared with saline treatment (Fig. 7C). No significant changes in body weight were observed between BAPN-treated and saline-treated mice during the study (Supplementary Fig. S5). Consistent with our findings that LOX activity drives collagen remodeling within the HGSOC tumor–mesothelial cocultures, BAPN-treated tumor omentum had significantly reduced collagen fiber amount compared with saline-treated tumor omentum as determined by SHG microscopy (Fig. 7D). These studies demonstrate that pharmacologic inhibition of LOX activity is an effective strategy to inhibit HGSOC progression and collagen remodeling in the metastatic HGSOC tumor microenvironment.

Discussion

Here we show that mesothelial cells are a cellular source of type I collagen in the HGSOC metastatic microenvironment and they facilitate HGSOC invasion through the secretion of the collagen remodeling enzyme LOX. Our data suggest a model where mesothelial cells lining the omentum interact with

Figure 6.
LOX expression by HGSOC tumor and mesothelial cells promotes collagen remodeling and invasion under hypoxic conditions. **A,** Quantification of the percentage volume of fiber amounts (top) and representative confocal collagen fiber images of 3D collagen gels (bottom) casted using conditioned media from OVCAR8 cultured alone, LP-9 cultured alone, and cocultures of OVCAR8 + LP-9 exposed to normoxia (21%) and hypoxia (2%) that were treated either with siRNA targeting LOX or siControl. Scale bar, 75 μm; $n = 3$. **B,** Graphical illustration of the percentage invasion and their representative images of OVCAR8 cells invading through Matrigel inserts primed with conditioned media from OVCAR8 cultured alone, LP-9 cultured alone, and cocultures of OVCAR8 + LP-9 exposed to normoxia (21%) and hypoxia (2%) that were treated either with siRNA pools targeting LOX or siControl. Scale bar, 75 μm; $n = 3$. Graph represents the normalized percentage of invading cells per field. Error bars, SD of the mean. *, $P < 0.05$.

disseminated HGSOC cancer cells in a hypoxic microenvironment. Hypoxia results in the stabilization of the hypoxic-inducible transcription factors HIF1 and HIF2 in both mesothelial and tumor cells. Hypoxic signaling preferentially upregulates the expression of factors involved in collagen biogenesis, stability (P4HA1, P4HA2, P4HA3, PLOD1, PLOD2) and collagen remodeling (LOX) within collagen type I expressing mesothelial cells to promote extracellular collagen deposition and remodeling. Hypoxic cancer cells further contribute to the remodeling of the extracellular collagen through the upregulation of LOX. Collectively, enhanced collagen type I remodeling by HGSOC tumor and mesothelial cells enhances HGSOC tumor invasion in a HIF- and LOX-dependent manner. These findings identify a role for mesothelial cells in collagen deposition and collagen remodeling within the HGSOC metastatic microenvironment.

Natarajan et al.
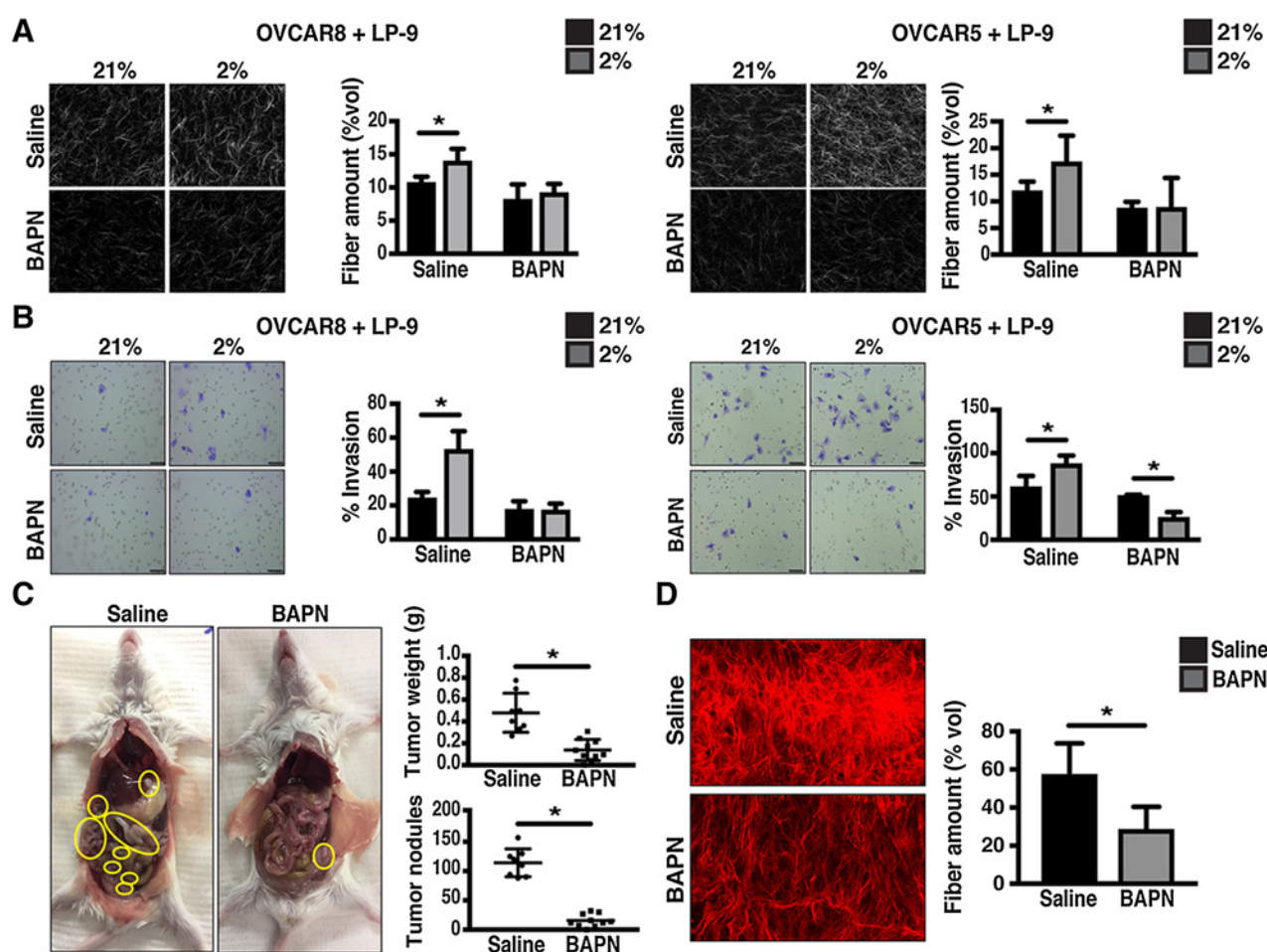
Figure 7.
Therapeutic inhibition of LOX inhibits metastatic ovarian cancer progression *in vivo*. **A,** Representative confocal images of collagen fibers from 3D collagen gels constructed using conditioned media from cocultures of OVCAR8 + LP-9 and OVCAR5 + LP-9 exposed to normoxic (21%) or hypoxic (2%) conditions treated with saline or the LOX inhibitor BAPN. Graphs show the corresponding quantification of the percentage volume of fiber amounts. Scale bar, 75 μm; $n = 3$.
B, Matrigel invasion assays of OVCAR8 or OVCAR5 cells through Matrigel inserts primed with conditioned media from cocultures of OVCAR8 + LP-9 or OVCAR5 + LP-9 exposed to normoxic (21%) or hypoxic (2%) conditions that were treated with saline or BAPN. Scale bar, 75 μm; $n = 3$. Graphs represent the normalized percentage of invading cells per field. **C,** Representative images showing metastatic tumor burden in 8-week-old female NSG mice that were intraperitoneally injected with OVCAR8 cells and treated either with saline or BAPN ($n = 8$ per treatment group). Graphical representation of tumor weight and tumor nodules in the mice administered with saline or BAPN. **D,** Representative SHG microscopy images of collagen fibrils from the omentum of mice that were injected intraperitoneally with OVCAR8 cells and treated with saline or BAPN. The graph shows MATLAB quantification of the percentage volume of fiber amount in the omentum of saline or BAPN-treated mice ($n = 2$ per treatment group; three ROIs per image were quantified). Error bars, SD of the mean. $*$, $P < 0.05$.

Collagen deposition and cross-linking plays an important role in metastatic tumor initiation and progression. Collagen deposition and remodeling in the extracellular matrix can directly promote tumor proliferation, evasion of growth suppression, death resistance, replicative immortality and invasion by engaging collagen receptors (DDR1, DDR2) as well as integrins (48). In addition, collagen deposition in the ECM can inhibit T-cell function and promote angiogenesis to facilitate tumor progression (48). In HGSOC, collagen-remodeling gene signatures are associated with metastasis and poor patient survival (34, 35). Grither and colleagues recently showed that the collagen receptor DDR2 is associated with poor survival in patients with HGSOC. Moreover, DDR2 signaling on HGSOC cells drives tumor cell mesothelial cell clearance, invasion through collagen type I, and metastasis *in vivo*, highlighting the importance of collagen recep-

tor signaling in mediating HGSOC tumor invasion and metastasis in the metastatic microenvironment (49). However, the cellular and molecular mechanisms driving collagen remodeling in the HGSOC metastatic microenvironment remains largely unknown. Here we demonstrate that mesothelial cells are a cellular source of collagen type I in the HGSOC metastatic microenvironment. Moreover, our findings suggest that the hypoxic tumor–mesothelial niche in HGSOC metastatic microenvironment may enhance collagen deposition and remodeling to facilitate the early stages of tumor cell invasion and metastasis.

Hypoxia and HIF signaling has a well-established role in promoting the hematogenous spread of cancer cells to distant tissue sites including the lung, liver, and bone. At these distant tissue sites, hypoxia and HIF signaling play an important role in establishing the premetastatic niche, modulation of tumor–

endothelial and endothelial–endothelial interactions to facilitate tumor extravasation from the vasculature, and metabolic adaptation of tumor cells (8). However, the role of hypoxia and HIF signaling in the transcoelomic spread of disseminated tumor cells within the peritoneal fluid to mesothelial lined peritoneal organs has not been investigated. Here we demonstrate that the HGSOC omental metastatic microenvironment is hypoxic where both tumor and mesothelial cells express HIF1 and HIF2 to facilitate the early stages of metastasis and tumor invasion. These findings identify an important role for hypoxia in mediating tumor–mesothelial interactions to support peritoneal metastasis.

Our findings have important clinical implications for the treatment of HGSOC. The overall survival rate of patients with HGSOC has not significantly changed over the past several decades (50). Surgery and platinum-based chemotherapy are the standard treatments for HGSOC. Despite the initial efficacy of these treatments, 80% of women diagnosed with advanced HGSOC will develop recurrent chemoresistant disease. For these reasons, efforts are focused on the development of targeted therapies to improve survival rates in women with advanced HGSOC. Our data suggest that anti-LOX treatment might be a clinically effective treatment strategy in HGSOC. The model of metastatic progression in our studies resembles the development of recurrent disease in patients with HGSOC following surgical debulking. We found that targeting LOX enzymatic activity as a single-agent therapy is sufficient to reduce peritoneal metastasis and collagen remodeling at the omentum in immunodeficient murine models of HGSOC. These findings suggest that anti-LOX–targeting agents may be an effective strategy to prevent or delay the development of tumor recurrence in metastatic HGSOC. In summary, our studies identify LOX as a druggable molecular target driving collagen remodeling and metastatic progression in HGSOC. These studies provide preclinical data to support the development of LOX inhibitors for the treatment of HGSOC.

Authors' Contributions

Conception and design: S. Natarajan, V. Krishnan, O. Dorigo, E.B. Rankin
Development of methodology: S. Natarajan, K.M. Foreman, N.S. Rossen, H. Shehade, V. Krishnan, S.C. Heilshorn, E.B. Rankin
Acquisition of data (provided animals, acquired and managed patients, provided facilities, etc.): S. Natarajan, K.M. Foreman, M.I. Soriano, N.S. Rossen, J.T. Eggold, O. Dorigo, K.C. Fuh, E.B. Rankin
Analysis and interpretation of data (e.g., statistical analysis, biostatistics, computational analysis): S. Natarajan, N.S. Rossen, D.R. Fregoso, J.T. Eggold, S.C. Heilshorn, S. Sinha, E.B. Rankin
Writing, review, and/or revision of the manuscript: S. Natarajan, V. Krishnan, O. Dorigo, S.C. Heilshorn, K.C. Fuh, E.B. Rankin
Administrative, technical, or material support (i.e., reporting or organizing data, constructing databases): S. Natarajan, D.R. Fregoso, A.J. Krieg
Study supervision: E.B. Rankin

References

1. Tan DS, Agarwal R, Kaye SB. Mechanisms of transcoelomic metastasis in ovarian cancer. Lancet Oncol 2006;7:925–34.
2. Iwanicki MP, Chen HY, Iavarone C, Zervantonakis IK, Muranen T, Novak M, et al. Mutant p53 regulates ovarian cancer transformed phenotypes through autocrine matrix deposition. JCI Insight 2016;1. doi: 10.1172/jci.insight.86829.
3. Iwanicki MP, Davidowitz RA, Ng MR, Besser A, Muranen T, Merritt M, et al. Ovarian cancer spheroids use myosin-generated force to clear the mesothelium. Cancer Discov 2011;1:144–57.
4. Davidowitz RA, Selfors LM, Iwanicki MP, Elias KM, Karst A, Piao H, et al. Mesenchymal gene program-expressing ovarian cancer spheroids exhibit enhanced mesothelial clearance. J Clin Invest 2014;124:2611–25.
5. Mikula-Pietrasik J, Sosinska P, Kucinska M, Murias M, Maksin K, Malinska A, et al. Peritoneal mesothelium promotes the progression of ovarian cancer cells *in vitro* and in a mice xenograft model *in vivo*. Cancer Lett 2014;355:310–5.
6. Kenny HA, Chiang CY, White EA, Schryver EM, Habis M, Romero IL, et al. Mesothelial cells promote early ovarian cancer metastasis through fibronectin secretion. J Clin Invest 2014;124:4614–28.
7. Rieppi M, Vergani V, Gatto C, Zanetta G, Allavena P, Taraboletti G, et al. Mesothelial cells induce the motility of human ovarian carcinoma cells. Int J Cancer 1999;80:303–7.
8. Rankin EB, Giaccia AJ. Hypoxic control of metastasis. Science 2016;352:175–80.
9. LaGory EL, Giaccia AJ. The ever-expanding role of HIF in tumour and stromal biology. Nat Cell Biol 2016;18:356–65.
10. Semenza GL. Hypoxia-inducible factors in physiology and medicine. Cell 2012;148:399–408.
11. Doedens AL, Stockmann C, Rubinstein MP, Liao D, Zhang N, DeNardo DG, et al. Macrophage expression of hypoxia-inducible factor-1 alpha suppresses T-cell function and promotes tumor progression. Cancer Res 2010;70:7465–75.
12. Imtiyaz HZ, Williams EP, Hickey MM, Patel SA, Durham AC, Yuan LJ, et al. Hypoxia-inducible factor 2alpha regulates macrophage function in mouse models of acute and tumor inflammation. J Clin Invest 2010;120:2699–714.
13. Chaturvedi P, Gilkes DM, Wong CC, Kshitiz, Luo W, Zhang H, et al. Hypoxia-inducible factor-dependent breast cancer-mesenchymal stem cell bidirectional signaling promotes metastasis. J Clin Invest 2013;123:189–205.
14. Kim JW, Evans C, Weidemann A, Takeda N, Lee YS, Stockmann C, et al. Loss of fibroblast HIF-1alpha accelerates tumorigenesis. Cancer Res 2012;72:3187–95.
15. Chi JT, Wang Z, Nuyten DS, Rodriguez EH, Schaner ME, Salim A, et al. Gene expression programs in response to hypoxia: cell type specificity and prognostic significance in human cancers. PLoS Med 2006;3:e47.
16. Osada R, Horiuchi A, Kikuchi N, Yoshida J, Hayashi A, Ota M, et al. Expression of hypoxia-inducible factor 1alpha, hypoxia-inducible factor 2alpha, and von Hippel-Lindau protein in epithelial ovarian neoplasms and allelic loss of von Hippel-Lindau gene: nuclear expression of hypoxia-inducible factor 1alpha is an independent prognostic factor in ovarian carcinoma. Hum Pathol 2007;38:1310–20.

17. Facciabene A, Peng X, Hagemann IS, Balint K, Barchetti A, Wang LP, et al. Tumour hypoxia promotes tolerance and angiogenesis via CCL28 and T (reg) cells. Nature 2011;475:226–30.

18. Ao Q, Su W, Guo S, Cai L, Huang L. SENP1 desensitizes hypoxic ovarian cancer cells to cisplatin by up-regulating HIF-1alpha. Sci Rep 2015;5: 16396.

19. Qin J, Liu Y, Lu Y, Liu M, Li M, Li J, et al. Hypoxia-inducible factor 1 alpha promotes cancer stem cells-like properties in human ovarian cancer cells by upregulating SIRT1 expression. Sci Rep 2017;7:10592.

20. Seo EJ, Kim DK, Jang IH, Choi EJ, Shin SH, Lee SI, et al. Hypoxia-NOTCH1-SOX2 signaling is important for maintaining cancer stem cells in ovarian cancer. Oncotarget 2016;7:55624–38.

21. Rupaimoole R, Ivan C, Yang D, Gharpure KM, Wu SY, Pecot CV, et al. Hypoxia-upregulated microRNA-630 targets Dicer, leading to increased tumor progression. Oncogene 2016;35:4312–20.

22. Roby KF, Taylor CC, Sweetwood JP, Cheng Y, Pace JL, Tawfik O, et al. Development of a syngeneic mouse model for events related to ovarian cancer. Carcinogenesis 2000;21:585–91.

23. Wilson C, Qiu L, Hong Y, Karnik T, Tadros G, Mau B, et al. The histone demethylase KDM4B regulates peritoneal seeding of ovarian cancer. Oncogene 2017;36:2565–76.

24. Gillette BM, Rossen NS, Das N, Leong D, Wang M, Dugar A, et al. Engineering extracellular matrix structure in 3D multiphase tissues. Biomaterials 2011;32:8067–76.

25. Rankin EB, Wu C, Khatri R, Wilson TL, Andersen R, Araldi E, et al. The HIF signaling pathway in osteoblasts directly modulates erythropoiesis through the production of EPO. Cell 2012;149:63–74.

26. Rankin EB, Fuh KC, Castellini L, Viswanathan K, Finger EC, Diep AN, et al. Direct regulation of GAS6/AXL signaling by HIF promotes renal metastasis through SRC and MET. Proc Natl Acad Sci U S A 2014;111:13373–8.

27. Li F, Lee KE, Simon MC. Detection of hypoxia and HIF in paraffin-embedded tumor tissues. Methods Mol Biol 2018;1742:277–82.

28. Brodsky AS, Fischer A, Miller DH, Vang S, MacLaughlan S, Wu HT, et al. Expression profiling of primary and metastatic ovarian tumors reveals differences indicative of aggressive disease. PLoS One 2014;9:e94476.

29. Arteel GE, Thurman RG, Raleigh JA. Reductive metabolism of the hypoxia marker pimonidazole is regulated by oxygen tension independent of the pyridine nucleotide redox state. Eur J Biochem 1998;253:743–50.

30. Jungermann K, Kietzmann T. Oxygen: modulator of metabolic zonation and disease of the liver. Hepatology 2000;31:255–60.

31. Barberis MC, Faleri M, Veronese S, Casadio C, Viale G. Calretinin. A selective marker of normal and neoplastic mesothelial cells in serous effusions. Acta Cytol 1997;41:1757–61.

32. Connell ND, Rheinwald JG. Regulation of the cytoskeleton in mesothelial cells: reversible loss of keratin and increase in vimentin during rapid growth in culture. Cell 1983;34:245–53.

33. Peters PN, Schryver EM, Lengyel E, Kenny H. Modeling the early steps of ovarian cancer dissemination in an organotypic culture of the human peritoneal cavity. J Vis Exp 2015:e53541. doi: 10.3791/53541.

34. Pearce OMT, Delaine-Smith RM, Maniati E, Nichols S, Wang J, Bohm S, et al. Deconstruction of a metastatic tumor microenvironment reveals a common matrix response in human cancers. Cancer Discov 2018;8: 304–19.

35. Cheon DJ, Tong Y, Sim MS, Dering J, Berel D, Cui X, et al. A collagen-remodeling gene signature regulated by TGF-beta signaling is associated with metastasis and poor survival in serous ovarian cancer. Clin Cancer Res 2014;20:711–23.

36. Junqueira LC, Bignolas G, Brentani RR. Picrosirius staining plus polarization microscopy, a specific method for collagen detection in tissue sections. Histochem J 1979;11:447–55.

37. Myllyharju J, Kivirikko KI. Collagens, modifying enzymes and their mutations in humans, flies and worms. Trends Genet 2004;20: 33–43.

38. Gilkes DM, Bajpai S, Chaturvedi P, Wirtz D, Semenza GL. Hypoxia-inducible factor 1 (HIF-1) promotes extracellular matrix remodeling under hypoxic conditions by inducing P4HA1, P4HA2, and PLOD2 expression in fibroblasts. J Biol Chem 2013;288:10819–29.

39. Myllyharju J, Schipani E. Extracellular matrix genes as hypoxia-inducible targets. Cell Tissue Res 2010;339:19–29.

40. Hofbauer KH, Gess B, Lohaus C, Meyer HE, Katschinski D, Kurtz A. Oxygen tension regulates the expression of a group of procollagen hydroxylases. Eur J Biochem 2003;270:4515–22.

41. Eisinger-Mathason TS, Zhang M, Qiu Q, Skuli N, Nakazawa MS, Karakasheva T, et al. Hypoxia-dependent modification of collagen networks promotes sarcoma metastasis. Cancer Discov 2013;3: 1190–205.

42. Gilkes DM, Semenza GL, Wirtz D. Hypoxia and the extracellular matrix: drivers of tumour metastasis. Nat Rev Cancer 2014;14:430–9.

43. Erler JT, Bennewith KL, Nicolau M, Dornhofer N, Kong C, Le QT, et al. Lysyl oxidase is essential for hypoxia-induced metastasis. Nature 2006;440: 1222–6.

44. Wong CC, Gilkes DM, Zhang H, Chen J, Wei H, Chaturvedi P, et al. Hypoxia-inducible factor 1 is a master regulator of breast cancer metastatic niche formation. Proc Natl Acad Sci U S A 2011;108:16369–74.

45. Barker HE, Cox TR, Erler JT. The rationale for targeting the LOX family in cancer. Nat Rev Cancer 2012;12:540–52.

46. Bignotti E, Tassi RA, Calza S, Ravaggi A, Bandiera E, Rossi E, et al. Gene expression profile of ovarian serous papillary carcinomas: identification of metastasis-associated genes. Am J Obstet Gynecol 2007;196: 245.

47. Ryner L, Guan Y, Firestein R, Xiao Y, Choi Y, Rabe C, et al. Upregulation of periostin and reactive stroma is associated with primary chemoresistance and predicts clinical outcomes in epithelial ovarian cancer. Clin Cancer Res 2015;21:2941–51.

48. Pickup MW, Mouw JK, Weaver VM. The extracellular matrix modulates the hallmarks of cancer. EMBO Rep 2014;15:1243–53.

49. Grither WR, Divine LM, Meller EH, Wilke DJ, Desai RA, Loza AJ, et al. TWIST1 induces expression of discoidin domain receptor 2 to promote ovarian cancer metastasis. Oncogene 2018;37:1714–29.

50. Bowtell DD, Bohm S, Ahmed AA, Aspuria PJ, Bast RC Jr, Beral V, et al. Rethinking ovarian cancer II: reducing mortality from high-grade serous ovarian cancer. Nat Rev Cancer 2015;15:668–79.

Cancer Research

AAGR American Association
for Cancer Research

Collagen Remodeling in the Hypoxic Tumor-Mesothelial Niche Promotes Ovarian Cancer Metastasis

Suchitra Natarajan, Kaitlyn M. Foreman, Michaela I. Soriano, et al.

Updated version	Access the most recent version of this article at: doi:10.1158/0008-5472.CAN-18-2616
Supplementary Material	Access the most recent supplemental material at: http://cancerres.aacrjournals.org/content/suppl/2019/03/12/0008-5472.CAN-18-2616.DC1

Visual Overview	**A diagrammatic summary of the major findings and biological implications:** http://cancerres.aacrjournals.org/content/79/9/2271/F1.large.jpg

Cited articles	This article cites 48 articles, 11 of which you can access for free at: http://cancerres.aacrjournals.org/content/79/9/2271.full#ref-list-1

E-mail alerts	Sign up to receive free email-alerts related to this article or journal.
Reprints and Subscriptions	To order reprints of this article or to subscribe to the journal, contact the AACR Publications Department at pubs@aacr.org.
Permissions	To request permission to re-use all or part of this article, use this link http://cancerres.aacrjournals.org/content/79/9/2271. Click on "Request Permissions" which will take you to the Copyright Clearance Center's (CCC) Rightslink site.